Cofactors

DOI: 10.1002/ange.201108827

Regulation of Redox Potential of a Pterin Derivative Bound to a Ruthenium(II) Complex by Intermolecular Hydrogen Bonding with Nucleobases**

Yuji Inui, Soushi Miyazaki, Kei Ohkubo, Shunichi Fukuzumi, and Takahiko Kojima**

Pterins are redox-active heteroaromatic coenzymes involved in a variety of redox-related reactions in biological systems to perform proton-coupled electron transfer (PCET).[1] They originate from guanosine triphosphate[2] and are fixed in the vicinity of metal ions by noncovalent interactions including hydrogen-bonding and π–π interactions to form active sites of metalloenzymes.[3] To realize a required functionality in a certain enzyme, the redox potential of the pterin cofactor needs to be appropriately regulated. For example, in the active site of heme-containing induced nitric oxide synthase (iNOS), tetrahydrobiopterin (H_4B) has π–π interaction with the indole ring of tryptophan 457 in the vicinity of the heme cofactor, which results in the stabilization of the radical intermediate of H_4B to facilitate electron transfer from H_4B to an $Fe–O_2$ complex.[4,5] Since the pterin cofactors are involved in extensive hydrogen-bonding networks in the active sites of pterin-dependent enzymes,[6] hydrogen bonding should be an important factor to regulate the redox potential. Any clear evidence, however, has yet to be provided to support the notion that hydrogen-bonding interaction exerted to the pterins is the critical factor for the regulation of their redox behavior. This is because the direct determination of the redox potentials of pterins is generally difficult in biological systems.[7] Thus, the lack of a sufficient dataset of redox potentials of pterins has precluded detailed discussion on the reactivity control of pterin-dependent enzymes by noncovalent interactions, which regulate the redox potentials of pterins in active sites of pterin-dependent enzymes.

Transition-metal complexes of pterin and their derivatives have been synthesized and characterized to demonstrate mainly their structures and redox behaviors.[8–11] Among the complexes, Ru^{II} complexes have been revealed to be useful for evaluating the redox potentials of the pterin ligand and for elucidating the PCET processes.[12,13] We have employed a Ru^{II}-TPA unit (TPA = tris(2-pyridylmethyl)amine) as a platform to obtain Ru^{II}-pterin complexes, which exhibited reversible redox waves for the pterin ligands to afford fairly stable radical species that were spectroscopically well-characterized.[13]

Herein, we demonstrate the first observation of redox potential control of pterin cofactors by hydrogen bonding on the Ru^{II}-TPA platform. We adopted the Ru^{II}-bound 6,7-dimethylpterin anion (dmp^-) of complex **1** (Figure 1) and ribonucleoside derivatives of guanosine, adenosine, and cytidine, and a deoxyribonucleoside derivative of thymidine, as hydrogen-bonding receptors (Figure 1).

We performed spectroscopic titration experiments of nucleoside derivatives into the solution of **1** in a mixed solvent of acetonitrile and chloroform to determine the binding constants.[14] In the ^1H NMR spectrum of **1** in $CDCl_3$/

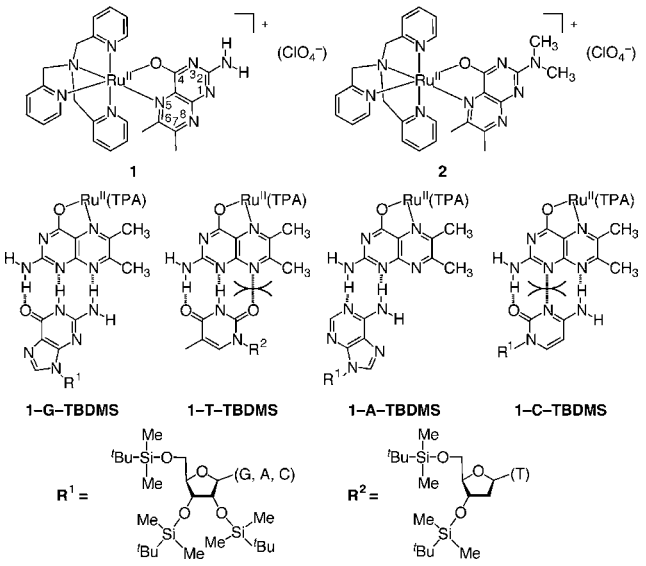

Figure 1. Structures of Ru-pterin-TPA complexes (**1** and **2**; top) and schematic description of plausible structures of hydrogen-bonding adducts between **1** and the nucleosides (middle). R denotes the sugar moiety in the corresponding nucleosides (bottom).

[*] Y. Inui, Dr. S. Miyazaki, Dr. K. Ohkubo, Prof. Dr. S. Fukuzumi
Department of Material and Life Science, Graduate School of Engineering, Osaka University, and ALCA (JST)
2-1 Yamada-oka, Suita, Osaka 565-0871 (Japan)
E-mail: fukuzumi@chem.eng.osaka-u.ac.jp
Prof. Dr. S. Fukuzumi
Department of Bioinspired Science, Ewha Womans University
Seoul 120-750 (Korea)
Prof. Dr. T. Kojima
Department of Chemistry, Graduate School of Pure and Applied Sciences, University of Tsukuba
1-1-1 Tennoudai, Tsukuba, Ibaraki 305-8571 (Japan)
E-mail: kojima@chem.tsukuba.ac.jp

[**] This work was supported by Grants-in-Aid (Nos. 23750014, 20108010, 21350035, and 20108001), a Global COE program, "The Global Education and Research Center for Bio-Environmental Chemistry" from the Japan Society of Promotion of Science (JSPS), the Ministry of Education, Science, and Technology of Japan, and by KOSEF/MEST through WCU project (R31-2008-000-10010-0) of Korea.

Supporting information for this article is available on the WWW under http://dx.doi.org/10.1002/anie.201108827.

© 2012 Wiley-VCH Verlag GmbH & Co. KGaA, Weinheim

CD_3CN (4:1, v/v), a singlet peak assigned to the 7-methyl group of the dmp^- ligand was observed at 2.83 ppm, which showed a gradual upfield shift in the course of the addition of G-TBDMS (Figure 1), as shown in Figure S1 in the Supporting Information.[15] Curve fitting of the change of the chemical shift relative to the concentration of G-TBDMS, as depicted in Figure S2(a) in the Supporting Information, allowed us to determine the binding constant as $1.0 \times 10^3\,M^{-1}$. The addition of T-TBDMS caused a slight upfield shift of the 7-methyl signal of the dmp^- ligand and the binding constant was estimated to be approximately $1 \times 10^2\,M^{-1}$ (Figure S2(b) in the Supporting Information). Concerning A-TBDMS and C-TBDMS, no significant change was observed even in the presence of about 50-fold excess of the nucleosides. These results indicate that the guanine part of G-TBDMS binds to the pterin ligand most strongly among the four nucleosides.

For the combination of the dmp^- ligand in **1** with the guanine, it is possible to form an adduct with three-point complementary hydrogen bonding, as depicted in Figure 1. This possibility has been clarified by the determination of the crystal structure of the hydrogen-bonding complex of 2-(isobutyrylamide)-6,7-dimethylpterin (Figure S3 in the Supporting Information) with 9-isopropylguanine, as shown in Figure 2, which clearly demonstrates a three-point hydrogen-bonding interaction between them.[16] On the basis of the crystal structure depicted in Figure 2, in the complementary hydrogen-bonding pair between complex **1** and the guanine part of G-TBDMS, the dmp^- ligand accepts two protons at the 1-N and 8-N positions, one of which is donated from the 2-amino group and the other from the 1-NH of the guanine part of G-TBDMS, and donates one proton of the 2-amino group of the dmp^- ligand to the carbonyl oxygen atom at the 6-position of the guanine part. The binding constant of G-TBDMS exhibited a linear correlation with T^{-1}, which allowed us to determine the enthalpy change ($\Delta H°$) upon the formation of the hydrogen-bonding complex to be -4.5 kcal mol^{-1} from the slope and the entropy change to be $-1.9\,cal\,mol^{-1}\,K^{-1}$ (Figure S5 in the Supporting Information). These values are comparable to those obtained for the formation of three-point hydrogen-bonding adducts of flavin derivatives with 2,6-bisamidepyridines.[17]

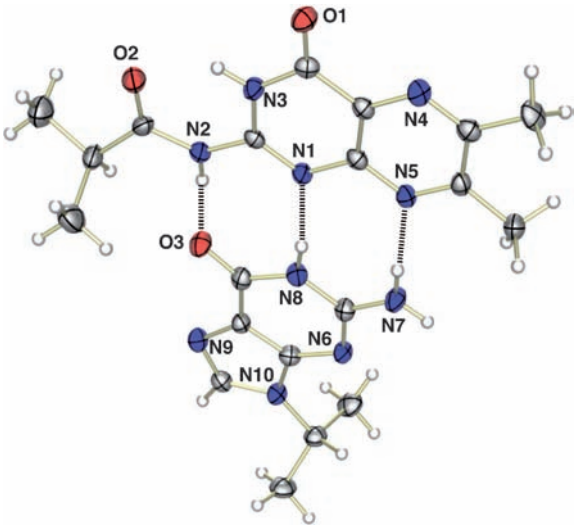

Figure 2. Crystal structure of the hydrogen-bonding complex between 2-(isobutyrylamide)-6,7-dimethylpterin and 9-isopropylguanine with 50% probability thermal ellipsoids. Dotted lines denote hydrogen bonds: N2···O3 2.767, N1···N8 2.957, N5···N7 2.988 Å.

As for the thymidine derivative, a two-point hydrogen-bonding interaction should be available with the 1-N and 2-NH_2 sites of the dmp^- ligand, as depicted in Figure 1. However, the lone pair of one of the two carbonyl oxygen atoms of the thymine part causes electrostatic repulsion with that of the 8-N nitrogen of the dmp^- ligand. DFT calculations suggested that, in the formation of a hydrogen-bonding adduct, the thymine plane should be tilted with a dihedral angle of 9° relative to the pterin mean plane to avoid the repulsion, as shown in Figure S6 in the Supporting Information. This may cause partial loss of stabilization of the hydrogen-bonding adduct to afford a small binding constant as mentioned above. Since the most basic site in the dmp^- ligand has been proved to be the 1-N position,[13c] hydrogen bonding to the 1-N position is favorable for the dmp^- ligand. From this viewpoint, G, T, and A should be favored because of their possibility to form at least two-point hydrogen bonding with the dmp^- ligand. However, the electrostatic repulsion between the lone pairs of 1-N of dmp^- and 3-N of the cytosine may avoid the close contact of the pterin ligand to the cytosine moiety of C-TBDMS. As can be seen in Figure 1, the adenine moiety of A-TBDMS is assumed to form two-point complementary hydrogen bonding at the 6-amino group and the 1-N atom with the 1-N and the 2-amino group of the pterin ligand, respectively; however, its binding constant is too low to be determined. We assume that the acidity of the 6-amino group of the adenine moiety is too weak to form a stable hydrogen-bonding adduct in a polar medium containing acetonitrile.[18]

We examined the importance of the 2-amino group of the dmp^- ligand in forming hydrogen bonds with the nucleobases by using complex **2** (Figure 1) bearing $dmdmp^-$ (Hdmdmp = *N*,*N*-dimethyl-6,7-dimethylpterin),[13] which has the *N*,*N*-dimethylamino group in place of the amino group at the 2-position, as a ligand. The singlet signal assigned to the 7-methyl group of the $dmdmp^-$ ligand of **2**, which was initially observed at 2.82 ppm, did not show any shift by addition of G-TBDMS, because the steric hindrance caused by the *N*,*N*-dimethylamino group of the $dmdmp^-$ ligand inhibited hydrogen bonding with nucleobases even for G-TBDMS. This difference between **1** and **2** clearly indicates the importance of the 2-amino group of the dmp^- ligand in the formation of hydrogen-bonding complexes with nucleobases.

Cyclic voltammetry (CV) and differential pulse voltammetry (DPV) were applied to determine the redox potentials of **1** with or without nucleoside derivatives in CH_3CN in the presence of 0.1 M tetra(*n*-butyl)ammonium hexafluorophosphate ($TBAPF_6$) as an electrolyte at room temperature under Ar. In the absence of the nucleosides, complex **1** showed a reversible redox wave at -1.63 V versus the saturated calomel electrode (SCE) due to the $dmp^-/dmp^{\bullet 2-}$ couple to produce $[Ru^{II}(dmp^{\bullet 2-})(TPA)]$ (the dotted line in Figure 3).[13]

© 2012 Wiley-VCH Verlag GmbH & Co. KGaA, Weinheim

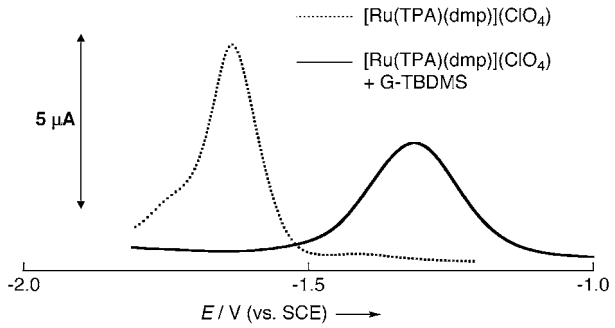

Figure 3. DPV traces for **1** (0.94 mM) in the absence (•••••) and presence (——) of 7.2 mM G-TBDMS in CH_3CN, in the presence of 0.1 M $TBAPF_6$ as an electrolyte under Ar at room temperature.

Table 1: Binding constants of the nucleosides and redox potentials of the $dmp^-/dmp^{\bullet 2-}$ couples.

Compound	K_{ox} [M^{-1}][a]	E_{red} [V][b]	ΔE_{red} [V]
1	–	−1.63[c]	–
1-G-TBDMS	1.0×10^3	−1.31	0.32
1-T-TBDMS	$\approx1\times10^2$	−1.42	0.21
1-C-TBDMS	<10	−1.60	0.03
1-A-TBDMS	<10	−1.62	0.01

[a] Determined by ^1H NMR measurements in $CDCl_3/CD_3CN$ (4:1, v/v) at room temperature. [b] Measured relative to $Ag/AgNO_3$ in CH_3CN at 293 K. The potentials were converted into values relative to the SCE by adding +0.29 V. The values were obtained by adding 7.7 equiv of G-TBDMS, 4.0 equiv of T-TBDMS, 12 equiv of C-TBDMS, and 9.1 equiv of A-TBDMS, relative to **1**. [c] Reversible. The value is presented as $E_{1/2}$.

Upon addition of a 7.7-fold excess amount of G-TBDMS, the redox wave in the CV trace showed a large positive shift and lost the reversibility (Figure S7(a) in the Supporting Information). The DPV measurement allowed us to determine the reduction potential of the dmp^- ligand to be −1.31 V versus SCE ($\Delta E_{red} = +0.32$ V; the solid line in Figure 3) in the hydrogen-bonding complex.

In the case of T-TBDMS, the addition of the nucleoside to the solution of **1** gave an anodic shift of the redox wave due to the $dmp^-/dmp^{\bullet 2-}$ couple from −1.63 to −1.42 V versus SCE ($\Delta E_{red} = +0.21$ V; Figure S8 in the Supporting Information). This suggests that the thymine moiety of T-TBDMS also strongly interacts with the reduced form of the dmp^- ligand ($dmp^{\bullet 2-}$), even though it does not bind so strongly to the dmp^- ligand. As for the addition of C- and A-TBDMS, the one-electron reduction potential exhibited only trivial shifts, at most +0.03 V for C-TBDMS and +0.01 V for A-TBDMS (Figure S9 in the Supporting Information). These results indicate that cytosine and adenine do not interact significantly with the pterin ligand, regardless of its reduction.

Binding constants of the nucleoside derivatives of **1** and redox potentials of the $dmp^-/dmp^{\bullet 2-}$ couple are summarized in Table 1. In comparison with the case of flavins,[6,19] the ΔE_{red} values obtained herein for the pterin complexes of G- and T-TBDMS are much larger. We attribute this difference of the hydrogen-bonding effects on the redox potentials between pterins and flavins to the positions in the coenzymes that form hydrogen bonds. Flavins have been reported to form hydrogen-bonding adducts at the 2-O, 3-NH, and O-4 positions,[6,17,19] which have little relationship with the PCET process of flavins. In contrast, in the cases of the pterin ligand in **1**, intermolecular hydrogen bonding can occur at the 8-N position that is involved in the PCET region (5-N, 6-C, 7-C, and 8-N) of pterin and forms the strongest hydrogen bonds with a hydrogen donor upon reduction of the pterin ligand in comparison with the 3- and 5-N positions.[13c] As an important point, it is only hydrogen bonding that modulates reduction potentials and protons are not completely transferred. This is an interesting facet of PCET chemistry and illustrates the importance of hydrogen bonding in the redox reactivity of biologically relevant cofactors.

To prove the formation of hydrogen bonds between the $dmp^{\bullet 2-}$ ligand and the nucleobases, we measured the ESR spectra of one-electron-reduced species of **1** as a probe by means of the chemical reduction of **1** (2.0 mM) with sodium naphthalenide ($Na(naph^{\bullet -})$) in the presence of the nucleosides (20 mM) at 243 K in CH_3CN. The one-electron-reduced species of **1** showed a well-resolved ESR signal at $g = 1.9991$, as shown in Figure 4a.[13b] Computer simulations of the spectrum allowed us to determine the hyperfine coupling (hfc) constants as 4.90 G for 5-N, 4.00 G for 8-N, 0.70 G for 6-

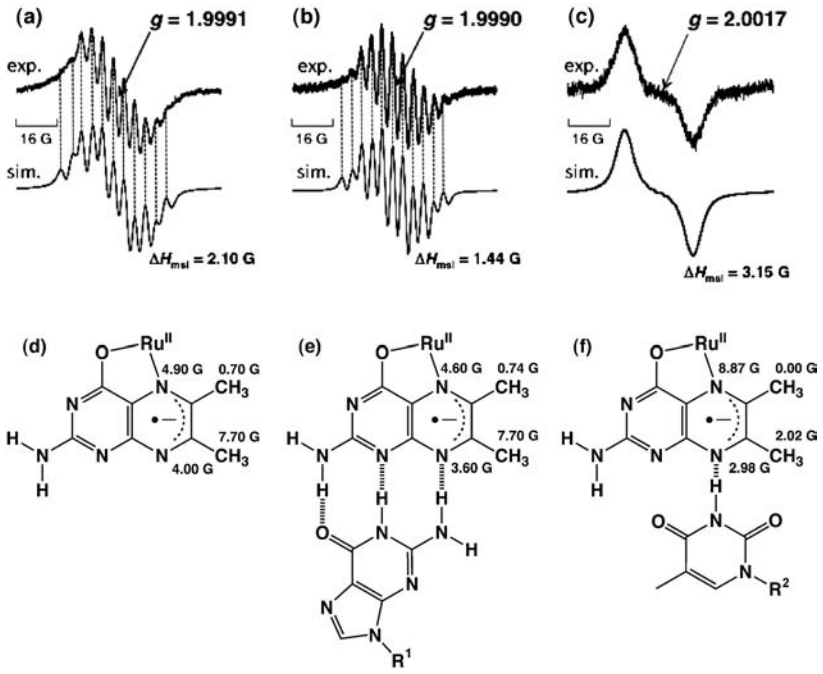

Figure 4. ESR spectra of the reduced species of **1** with their computer simulations (a) and those in the presence of G-TBDMS (b) and T-TBDMS (c), in deaerated CH_3CN at 243 K. Estimated hfc values with computer simulations are included (d–f). ΔH_{msl} denotes the mid-slope line width for the simulation.

© 2012 Wiley-VCH Verlag GmbH & Co. KGaA, Weinheim

CH_3, and 7.70 G for 7-CH_3, as shown in Figure 4d. These results indicate that the unpaired electron is delocalized in the PCET region as observed in other related Ru-bound pterin radical species.[13]

DFT calculations on the dmp$^{\bullet 2-}$ π-radical dianion were also performed at the B3LYP/6-31G(d) level of theory to estimate the hfc constants (Figure S10 in the Supporting Information). The ESR spectrum of the reduced species of **1** in the presence of G-TBDMS exhibited a well-resolved ESR signal at $g = 1.9990$ with hyperfine splitting (Figure 4b), and the simulation afforded hfc constants of 4.60 G for 5-N, 3.60 G for 8-N, 0.74 G for 6-CH_3, and 7.70 G for 7-CH_3, as shown in Figure 4e. The values for 5-N and 8-N became smaller by the addition of G-TBDMS than those of the dmp$^{\bullet 2-}$ π-radical dianion of **1**. This tendency was also confirmed by DFT calculations and is caused by delocalization of an unpaired electron in a wider region: this delocalization can be attained as a result of the intermolecular hydrogen bonding between G-TBDMS and the dmp$^{\bullet 2-}$ π-radical dianion ligand. This indicates that the hydrogen bonding alters the distribution of the unpaired electron, as in the case of flavins and their derivatives.[19]

In the case of T-TBDMS, the ESR spectrum of the reduced species of **1** changed dramatically to show an ESR signal at $g = 2.0017$ (see Figure 4c). Simulation of the spectrum allowed us to estimate hfc constants of 8.87 G for 5-N and 2.98 G for 8-N. Comparison of the hfc constants clearly indicates that thymine binds to the dmp$^{\bullet 2-}$ π-radical dianion in a different hydrogen-bonding mode from that of the guanine. The hydrogen bond formation ability of T-TBDMS is assumed to occur only at the 8-N position of the dmp$^{\bullet 2-}$ ligand, as supported by the fact that a proton shift occurs from 1-N to 8-N in the course of one-electron reduction of protonated [Ru(TPA)(Hdmp)]$^{2+}$, where the proton initially resides at the 1-N position.[13c] Once the dmp$^-$ ligand is reduced, the spin density is delocalized onto the N5-C6-C7-N8 region,[13] whereas in the one-electron-reduced species of the protonated complex **1**, the proton goes to the 8-N position to stabilize the radical species.[13c] This suggests that the hydrogen bonding at the 8-N position should be strengthened in the reduced form due to the increase of the negative charge at the 8-N position of the dmp$^{\bullet 2-}$ ligand. Since the pK_a values of the 3-N*H* of guanine and that of thymine have been reported to be 9.2–9.6 and 9.9, respectively,[18] the ΔH value of single-point hydrogen bonding at the 3-N*H* should be virtually the same for both the nucleobases in an electrostatic sense.

These arguments suggest that the large positive shift of the reduction potential of the dmp$^-$ ligand in the presence of T-TBDMS may stem from the change of binding mode: the thymine moiety which binds to the 1-N and 2-NH_2 positions of the dmp$^-$ ligand shifts to form a single-point hydrogen bond to the 8-N position of the dmp$^{\bullet 2-}$ ligand in the DFT-optimized structure of the one-electron-reduced species of **1** with the imido N-H group of thymine, as shown in Figure 5, similar to the proton shift mentioned above.[13c] The DFT-optimized structure of the one-electron-reduced species of the Hdmp$^{\bullet -}$-(1-methylthymine) adduct is depicted in Figure 5, and the dihedral angle between the Hdmp$^{\bullet -}$ ligand and the thymine plane is estimated to be 65° (see also Figure S6 in the Supporting Information). Thus, the results of DFT calculations also suggest a hydrogen-bond shift of the thymine moiety as shown in Figure 5. The compensation of the attractive interaction (hydrogen bonding) and the electrostatic repulsion between the carbonyl oxygen atoms and the π-electron clouds of the aromatic ring of the pterin ligand had a weaker impact on the redox potential of the pterin ligand than that of the complementarily stabilized guanine adduct.

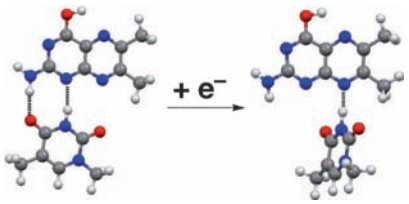

Figure 5. DFT-optimized structures of hydrogen-bonding adducts of Hdmp$^{\bullet -}$-1-methylthymine at the B3LYP/6-31G(d) level of theory.

In summary, we have clearly demonstrated for the first time the modulation of redox potential of a pterin coenzyme by intermolecular hydrogen bonding with the aid of the Ru^{II}-TPA coordination environment. The pterin ligand undergoes complementary three-point hydrogen bonding with the guanine derivative at the 2-NH_2, 1-N, and 8-N positions of the dmp$^-$ ligand, as clarified by X-ray crystallography on a complex made of 2-(isobutyrylamide)-6,7-dimethylpterin and 9-isopropylguanine, which results in a large anodic shift of the reduction potential of the dmp$^-$ ligand of +0.32 V. The thymine derivative forms probably two-point intermolecular hydrogen bonds with the dmp$^-$ ligand at the 1-N and 2-NH_2 sites, and shows a tenfold smaller binding constant than that of the guanine derivative. The thymidine derivative also induced a fairly large positive shift (+0.21 V) of the reduction potential of the dmp$^-$ ligand. This positive shift is probably derived from a strong single-point hydrogen bond between the 8-N position of the pterin and the 3-N*H* of the thymine moiety through "proton shift" in the course of the reduction of the pterin ligand. In consequence, the hydrogen bonding toward the 8-N position of pterins, which is involved in the PCET region (5-N, 6-C, 7-C, and 8-N), causes a significant modulation of their redox potentials.

Received: December 15, 2011
Published online: March 30, 2012

Keywords: cofactors · hydrogen bonds · nucleobases · redox chemistry · ruthenium

[1] C.-C. Wei, B. R. Crane, D. J. Stuehr, *Chem. Rev.* **2003**, *103*, 2365–2383.
[2] a) B. Thöny, G. Auerbach, N. Blau, *Biochem. J.* **2000**, *347*, 1–16; b) G. Basset, E. P. Quinlivan, M. J. Ziemak, R. Díaz de la Garza, M. Fisher, S. Schiffmann, A. Bacher, J. F. Gregory III, A. D. Hanson, *Proc. Natl. Acad. Sci. USA* **2002**, *99*, 12489–12494.
[3] C.-C. Wei, Z.-Q. Wang, A. S. Arvai, C. Hemann, R. Hille, E. D. Getzoff, D. J. Stuehr, *Biochemistry* **2003**, *42*, 1969–1977.

 © 2012 Wiley-VCH Verlag GmbH & Co. KGaA, Weinheim

[4] Z.-Q. Wang, C.-C. Wei, S. Ghosh, A. L. Meade, C. Hemann, R. Hille, D. J. Stuehr, *Biochemistry* **2001**, *40*, 12819 – 12825.
[5] M. Aoyagi, A. S. Arvai, S. Ghosh, D. J. Stuehr, J. A. Tainer, E. D. Getzoff, *Biochemistry* **2001**, *40*, 12826 – 12832.
[6] a) S. Leimkühler, M. M. Wuebbens, K. V. Rajagopalan, *Coord. Chem. Rev.* **2011**, *255*, 1129 – 1144.
[7] A. C. F. Gorren, A. J. Kungl, K. Schmidt, E. R. Werner, B. Mayer, *Nitric Oxide: Biol. Chem.* **2001**, *5*, 176 – 186.
[8] For Mo: a) B. Fischer, J. Strähle, M. Viscontini, *Pteridines* **1992**, *3*, 91 – 93; b) B. Fischer, H. Schmalle, E. Dubler, A. Schäfer, M. Viscontini, *Inorg. Chem.* **1995**, *34*, 5726 – 5734; c) B. Fischer, H. W. Schmalle, M. R. Baumgartner, M. Viscontini, *Helv. Chim. Acta* **1997**, *80*, 103 – 110.
[9] For Mo: a) S. J. N. Burgmayer, M. R. Arkin, L. Bostick, S. Dempster, K. M. Everett, H. L. Layton, K. E. Paul, C. Rogge, A. L. Rheingold, *J. Am. Chem. Soc.* **1995**, *117*, 5812 – 5823; b) H. L. Kaufmann, L. Liable-Sands, A. L. Rheingold, S. J. N. Burgmayer, *Inorg. Chem.* **1999**, *38*, 2592 – 2599; c) H. L. Kaufmann, P. J. Carroll, S. J. N. Burgmayer, *Inorg. Chem.* **1999**, *38*, 2600 – 2606; d) S. J. N. Burgmayer, H. L. Kaufmann, G. Fortunato, P. Hug, B. Fischer, *Inorg. Chem.* **1999**, *38*, 2607 – 2613.
[10] R. S. Pilato, K. A. Eriksen, M. A. Greaney, E. I. Stiefel, S. Goswami, L. Kilpatrick, T. G. Spiro, E. C. Tayler, *J. Am. Chem. Soc.* **1991**, *113*, 9372 – 9374.
[11] For Cu: a) T. Kohzuma, H. Masuda, O. Yamauchi, *J. Am. Chem. Soc.* **1989**, *111*, 3431 – 3433; b) A. Odani, H. Masuda, K. Inukai, O. Yamauchi, *J. Am. Chem. Soc.* **1992**, *114*, 6294 – 6300; c) J. Perkinson, S. Brodie, K. Yoon, K. Mosny, P. J. Carroll, T. V. Morgan, S. J. N. Burgmayer, *Inorg. Chem.* **1991**, *30*, 719 – 727; d) M. Mitsumi, J. Toyoda, K. Nakasuji, *Inorg. Chem.* **1995**, *34*, 3367 – 3370; e) D.-H. Lee, N. N. Murthy, Y. Lin, N. S. Nasir, K. D. Karlin, *Inorg. Chem.* **1997**, *36*, 6328 – 6334; Other metal ions: Y. Funahashi, Y. Hara, H. Masuda, O. Yamauchi, *Inorg. Chem.* **1997**, *36*, 3869 – 3875.
[12] A. Abelleira, R. D. Galang, M. J. Clarke, *Inorg. Chem.* **1990**, *29*, 633 – 639.
[13] a) T. Kojima, T. Sakamoto, Y. Matsuda, K. Ohkubo, S. Fukuzumi, *Angew. Chem.* **2003**, *115*, 5101 – 5104; *Angew. Chem. Int. Ed.* **2003**, *42*, 4951 – 4954; b) S. Miyazaki, T. Kojima, T. Sakamoto, T. Mastumoto, K. Ohkubo, S. Fukuzumi, *Inorg. Chem.* **2008**, *47*, 333 – 343; c) S. Miyazaki, K. Ohkubo, T. Kojima, S. Fukuzumi, *Angew. Chem.* **2008**, *120*, 9815 – 9818; *Angew. Chem. Int. Ed.* **2008**, *47*, 9669 – 9672; d) S. Fukuzumi, T. Kojima, *J. Biol. Inorg. Chem.* **2008**, *13*, 321 – 333; e) S. Miyazaki, T. Kojima, J. M. Mayer, S. Fukuzumi, *J. Am. Chem. Soc.* **2009**, *131*, 11615 – 11624.
[14] In the ^{1}H NMR spectra of the mixtures of the nucleosides with **1**, the signals derived from the ribose moieties did not show any spectral change from those of the original spectra. Thus, we concluded that the ribose moiety is not involved in the adduct formation with the pterin ligands.
[15] Similar upfield shift in hydrogen bond formation has been reported: S. Goswami, N. K. Das, D. Sen, G. Hazra, J. H. Goh, Y. C. Sing, H.-K. Fun, *New J. Chem.* **2011**, *35*, 2811 – 2819.
[16] For details including the numbering scheme (Figure S4(a)) and a view of the crystal packing (Figure S4(b)), see the Supporting Information. Crystallographic data for $C_{22}H_{34}N_{10}O_5$: monoclinic; $P2_1/a$; $a = 7.681(3)$, $b = 28.221(12)$, $c = 11.598(5)$ Å; $\beta = 104.335(6)°$; $V = 2511.4(18)$ Å^3; $T = 120(2)$ K; $Z = 4$; $R1(R_w) = 0.0725(0.1724)$ ($I > 2\sigma(I)$); GOF = 0.997. CCDC 849641 contains the supplementary crystallographic data for this paper. These data can be obtained free of charge from The Cambridge Crystallographic Data Centre via www.ccdc.cam.ac.uk/data_request/cif.
[17] A. J. Goodman, E. C. Breinlinger, C. M. McIntosh, L. N. Grimaldi, V. M. Rotello, *Org. Lett.* **2001**, *3*, 1531 – 1534.
[18] V. Verdolino, R. Cammi, B. H. Munk, H. B. Schlegel, *J. Phys. Chem. B* **2008**, *112*, 16860 – 16873, and references therein.
[19] S. Miyazaki, K. Ohkubo, T. Kojima, S. Fukuzumi, *Angew. Chem.* **2007**, *119*, 923 – 926; *Angew. Chem. Int. Ed.* **2007**, *46*, 905 – 908.

 © 2012 Wiley-VCH Verlag GmbH & Co. KGaA, Weinheim